NONLINEAR BEHAVIOR OF POWER HBT

Woonyun Kim*, Sanghoon Kang**, Kyungho Lee**, Minchul Chung**, and Bumman Kim**

*RFIC Design Team, System LSI Division, Samsung Electronics Co., Ltd., San 24, Nongseo-Lee, Kiheung-Eup, Yongin-Si, Kyungki-Do, 449-711, Korea.
Phone: +82-54-279-5584, Fax: +82-54-279-2903, E-mail: kwn@postech.ac.kr
**Dept. of E. E. Eng. and MARC, POSTECH, San 31, Hyoja-Dong, Pohang, Kyungbuk, 790-784, Korea.

Abstract— **To understand the linear characteristics of HBT more accurately, an analytical nonlinear HBT model using Volterra Series analysis is developed. The model considers four nonlinear components: r_π, C_{diff}, C_{depl}, and g_m. It shows that nonlinearities of r_π and C_{diff} are almost completely cancelled by g_m nonlinearity at all frequencies. The residual g_m nonlinearity are highly degenerated by the input impedances. Therefore, r_π, C_π and g_m nonlinearities generate less IM3 than C_{bc}. If C_{bc} is linearized, C_{depl} and g_m are the main nonlinear sources of HBT, and C_{depl} becomes very important at a high frequency. It was also found that the degeneration resistor, R_E, is more effective than R_B for reducing g_m nonlinearity. This analysis also provides the dependency of the source second harmonic impedance on the linearity of HBT. The IM3 of HBT is significantly reduced by setting the second harmonic impedance of $Z_{S,2\omega_2} = 0$ and $Z_{S,\omega_2-\omega_1} = 0$.**

I. Introduction

The transmitter of the handset of digital mobile communication systems requires highly efficient linear power amplifiers [1–4]. HBTs are widely used for the amplifiers and their nonlinear behavior has been extensively measured and analyzed [4–12]. It is commonly known that C_{bc} is the dominant nonlinear source and should be linearized to reduce the intermodulation distortions [7, 9–13]. C_{bc} is a depletion capacitance and it is rather moderate nonlinear component. It is surprising in view of the fact that HBT has highly nonlinear sources. The dependence of the HBT's base current, i_B, on base-to-emitter voltage, v_{BE}, is an exponential function, one of the strongest nonlinearities found in nature. So is its collector current, i_C, which is basically similar to i_B. Furthermore, the junction capacitance, primarily a diffusion capacitance, is also strongly nonlinear. These exponential nonlinear behaviors are not seen in the nonlinear characteristics of HBTs. Thus, the measured high linear characteristics of HBT has motivated many researchers to study intermodulation (IM) mechanism of HBT. The good linearity of HBT's was attributed to the partial cancellation between IM currents generated from the exponential junction current and the junction capacitance [5], or the partial cancellation of IM currents from the total base-emitter current and the total base-collector current [8]. According to reference [9], the high linear characteristis of HBT resulted from the almost complete cancellation between the output nonlinear current components generated by emitter-base current source and base-collector current source. It was also reported that the emitter and base resistances linearize the HBT output [10]. Because of the different descriptions for the linear characteristics, a more complete explanation is needed.

To understand the linear characteristics of HBT more accurately, we have developed an analytical nonlinear HBT model using Volterra Series analysis [14]. The presented analysis describes the fundamental nonlinear behavior of HBT.

II. The Nonlinear Model of HBT

The simplified equivalent circuit of HBT used for the analysis is shown in Fig. 1. The emitter and base resistances are R_E and R_B, respectively. These resistances are linear components. The base and collector nonlinear current source are represented as i_B and i_C, respectively. And, the base-emitter nonlinear capacitance is appeared as a charge, q_{BE}. C_{BC} is assumed to be linearized for a constant capacitance and is omitted for the nonlinear circuit analysis. Z_S and Z_L represent the source and load impedances, respectively. The source is conjugate-matched for the maximum gain. This model includes all important nonlinearities and is good enough for representing essential nonlinear properties of HBT.

The nonlinear elements are represented by the third-order expansion of Taylor series. Under a small-signal condition, the base nonlinear current source can be expanded at the vicinity of its bias point. The i_B is modeled as

$$
\begin{aligned}
i_B &= I_{SB}\left[\exp\left(\frac{v_{BE}}{\eta_B V_T}\right) - 1\right] && (1)\\
i_b &= \frac{I_B}{\eta_B V_T} v_{be} + \frac{I_B}{2\eta_B^2 V_T^2} v_{be}^2 + \frac{I_B}{6\eta_B^3 V_T^3} v_{be}^3 && (2)\\
&\equiv g_1 v_{be} + g_2 v_{be}^2 + g_3 v_{be}^3 && (3)
\end{aligned}
$$

where I_{SB} represents the saturation current, η_B is the ideality factor of the base current, I_B is dc base current, and V_T is thermal voltage. i_b and v_{be} are the small-signal components of i_B and v_{BE}, respectively. Also the coefficient $g_1 = 1/r_\pi$ is a linear junction conductance.

i_C is also modeled as

$$i_C = I_{SC}\left[\exp\left(\frac{v_{BE}}{\eta_C V_T}\right) - 1\right] \qquad (4)$$

where I_{SC} represents the saturation current, η_C is the ideality factor of the collector current. It can be expanded at the vicinity of its bias point, yielding

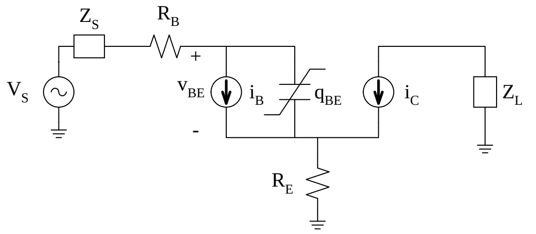

Fig. 1. HBT nonlinear equivalent model

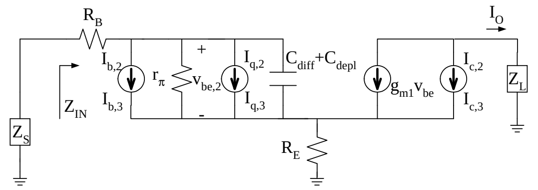

Fig. 2. HBT equivalent circuit for the 2nd- and 3rd-order intermodulation analysis.

$$
\begin{aligned}
i_c &= \frac{I_C}{\eta_C V_T} v_{be} + \frac{I_C}{2\eta_C^2 V_T^2} v_{be}^2 + \frac{I_C}{6\eta_C^3 V_T^3} v_{be}^3 && (5)\\
&\equiv g_{m1} v_{be} + g_{m2} v_{be}^2 + g_{m3} v_{be}^3 && (6)
\end{aligned}
$$

where I_C is dc collector current, and i_c is the small-signal component of i_C. The coefficient, g_{m1} is generally called g_m. The common emitter current gain (β_{ac}) can be calculated by g_{m1}/g_1.

The stored charge at the base-emitter junction, q_{BE}, is the sum of diffusion charge and depletion charge.

$$
\begin{aligned}
q_{BE} &= \tau_B i_C + \tau_E i_B + q A_E X_N N_E && (7)\\
q_{be} &= \left(\frac{I_C}{\eta_C V_T} \tau_B + \frac{I_B}{\eta_B V_T} \tau_E + C_{jE} \right) v_{be} \\
&+ \left(\frac{I_C}{2\eta_C^2 V_T^2} \tau_B + \frac{I_B}{2\eta_B^2 V_T^2} \tau_E + \frac{C_{jE}}{4(V_{bi} - V_{BE})} \right) v_{be}^2 \\
&+ \left(\frac{I_C}{6\eta_C^3 V_T^3} \tau_B + \frac{I_B}{6\eta_B^3 V_T^3} \tau_E + \frac{C_{jE}}{8(V_{bi} - V_{BE})^2} \right) v_{be}^3 && (8)\\
&\equiv c_1 v_{be} + c_2 v_{be}^2 + c_3 v_{be}^3 && (9)
\end{aligned}
$$

where τ_B is the base transit time of the minority carrier in base, and τ_E is the transit time of the minority carrier in the emitter, and is assumed to be comparable to τ_B. A_E is the emitter area, X_N is the depletion width of the emitter, and N_E is the doping concentration of the emitter. q_{be} is the small-signal component of q_{BE}, $C_{jE} = A_E \sqrt{\frac{q\epsilon_E \epsilon_B N_E P_B}{2(\epsilon_E N_E + \epsilon_B P_B)(V_{bi} - V_{BE})}}$, and C_{diff} is $\frac{I_C}{\eta_C V_T}\tau_B + \frac{I_B}{\eta_B V_T}\tau_E$. For simplicity, depletion approximation has been used. V_{bi} is built-in potential of base-emitter junction and V_{BE} is the base-emitter dc voltage. c_1 is so-called the base-emitter junction capacitance, C_π.

III. The Second Order Harmonic Analysis

The first-order equation for the base-to-emitter voltage V_{be,ω_q} at the excitation frequency ω_q can be expressed by

$$
V_{be,\omega_q} = \frac{Z_{\pi,\omega_q}}{Z_{IN,\omega_q} + Z_{S,\omega_q}} V_{S,\omega_q} \qquad (10)
$$

where $Z_{\pi,\omega_q} = \frac{1}{g_1 + j\omega_q c_1}$, Z_{IN,ω_q} ($= R_B + Z_{\pi,\omega_q} + R_E(1 + g_{m1} Z_{\pi,\omega_q})$) is the input impedance of the HBT, and the source impedance, Z_{S,ω_q} is conjugately matched to Z_{IN,ω_q}. The harmonics can be found by means of Volterra Series analysis. Fig. 2 shows the equivalent circuit for the second- and third-order nonlinear analysis. The second-order intermodulation current generated by the nonlinear base-emitter junction capacitance, $I_{q,2}$, and by the nonlinear base and collector current sources, $I_{b,2}$ and $I_{c,2}$ are given by

$$
\begin{aligned}
I_{q,2\omega_2} &= \frac{1}{2} j(2\omega_2) c_2 V_{be,\omega_2}^2 = j\omega_2 c_2 V_{be,\omega_2}^2, && (11)\\
I_{b,2\omega_2} &= \frac{1}{2} g_2 V_{be,\omega_2}^2, && (12)\\
I_{c,2\omega_2} &= \frac{1}{2} g_{m2} V_{be,\omega_2}^2. && (13)
\end{aligned}
$$

Performing a linear analysis of this circuit, we find the base-emitter junction voltage at the second harmonic;

$$
\begin{aligned}
V_{be,2\omega_2} &= \frac{-(Z_{S,2\omega_2} + R_B + R_E) Z_{\pi,2\omega_2} (I_{b,2\omega_2} + I_{q,2\omega_2})}{Z_{IN,2\omega_2} + Z_{S,2\omega_2}} \\
&- \frac{R_E Z_{\pi,2\omega_2} I_{c,2\omega_2}}{Z_{IN,2\omega_2} + Z_{S,2\omega_2}} && (14)
\end{aligned}
$$

The output current $I_{O,2\omega_2}$ at this second-harmonic frequency is

$$
I_{O,2\omega_2} = g_{m1} V_{be,2\omega_2} + I_{c,2\omega_2} \qquad (15)
$$

Substituting (14) into (15), $\frac{R_E g_{m1} Z_{\pi,2\omega_2}}{Z_{IN,2\omega_2} + Z_{S,2\omega_2}} I_{c,2\omega_2}$ is cancelled out by the $g_{m1} R_E$ feedback term in the last term of (14). The remain terms of the above equation is simplified as

$$
\begin{aligned}
I_{O,2\omega_2} &= Z_A \{ -g_{m1} I_{b,2\omega_2} + g_1 I_{c,2\omega_2} \} \\
&+ Z_A \{ -g_{m1} I_{q,2\omega_2} + j2\omega_2 c_1 I_{c,2\omega_2} \} \\
&+ \frac{Z_{\pi,2\omega_2}}{Z_{IN,2\omega_2} + Z_{S,2\omega_2}} I_{c,2\omega_2} && (16)
\end{aligned}
$$

where Z_A is $\frac{(Z_{S,2\omega_2} + R_B + R_E) Z_{\pi,2\omega_2}}{Z_{IN,2\omega_2} + Z_{S,2\omega_2}}$.

$$
\begin{aligned}
I_{O,2\omega_2} &= Z_A \frac{g_m}{2r_\pi} \left(\frac{1}{2V_T \eta_C} - \frac{1}{2V_T \eta_B} \right) V_{be,\omega_2}^2 \\
&+ Z_A j\omega_2 g_m \frac{C_{diff}}{(\beta_{ac} + 1)} \left(\frac{1}{2\eta_C V_T} - \frac{1}{2\eta_B V_T} \right) V_{be,\omega_2}^2 \\
&+ Z_A j\omega_2 g_m C_{jE} \left(\frac{1}{2\eta_C V_T} - \frac{1}{4(V_{bi} - V_{BE})} \right) V_{be,\omega_2}^2 \\
&+ \frac{Z_{\pi,2\omega_2}}{Z_{IN,2\omega_2} + Z_{S,2\omega_2}} \frac{g_m}{4\eta_C V_T} V_{be,\omega_2}^2 && (17)
\end{aligned}
$$

The first term in (17) originates from the cancellation of r_π and g_m nonlinearities which have exponential forms. If the ideality factors of the current sources are identical, the second order IM distortion generated from the nonlinear base current source (r_π) can be completely removed by a portion of the nonlinear distortion generated from the collector current source (g_m). The second term shows the cancellation between C_{diff} and g_m nonlinearities. The second term of (17) has the nonlinear term from the diffusion capacitance, which is reduced by a factor of $1/(\beta_{ac} + 1)$ and can again be completely removed by matching the ideality factors of the current sources. The third term generated from the base-emitter depletion capacitance can be cancelled by some portion of that generated from i_C, but can not be completely eliminated due to the different origin of sources. The last term is the remained g_m nonlinear portion. The coefficient $\frac{Z_{\pi,2\omega_2} g_m}{Z_{IN,2\omega_2}+Z_{S,2\omega_2}}$ of the last term is identical to the degenerated g_m nonlinearity equation at a low frequency. In summary, the r_π and C_{diff} nonlinearities almost completely cancelled by g_m nonlinearity and C_{depl} nonlinearity is partially removed by g_m nonlinearity. The remained g_m nonlinear component is quite similar to the low frequency case with large degeneration resistances.

IV. The Third Order Analysis

We have performed a similar analysis for the third order Intermodulation. From a similar sequence to the second order analysis, the third order output current, $I_{O,2\omega_2-\omega_1}$ is given by

$$
\begin{aligned}
\mathbf{I_{O,2\omega_2-\omega_1}} &= \frac{(Z_{S,2\omega_2-\omega_1}+R_B+R_E)Z_{\pi,2\omega_2-\omega_1}}{Z_{IN,2\omega_2-\omega_1}+Z_{S,2\omega_2-\omega_1}}\frac{g_m}{r_\pi} \\
&\left[\left(\frac{1}{8\eta_C^2V_T^2}-\frac{1}{8\eta_B^2V_T^2}\right)+A\left(\frac{1}{2\eta_C V_T}-\frac{1}{2\eta_B V_T}\right)\right]B \\
&+\frac{(Z_{S,2\omega_2-\omega_1}+R_B+R_E)Z_{\pi,2\omega_2-\omega_1}}{Z_{IN,2\omega_2-\omega_1}+Z_{S,2\omega_2-\omega_1}}g_m j(2\omega_2-\omega_1)\frac{C_{diff}}{(1+\beta_{ac})} \\
&\left[\left(\frac{1}{8\eta_C^2V_T^2}-\frac{1}{8\eta_B^2V_T^2}\right)+A\left(\frac{1}{2\eta_C V_T}-\frac{1}{2\eta_B V_T}\right)\right]B \\
&+\frac{(Z_{S,2\omega_2-\omega_1}+R_B+R_E)Z_{\pi,2\omega_2-\omega_1}}{Z_{IN,2\omega_2-\omega_1}+Z_{S,2\omega_2-\omega_1}}g_m j(2\omega_2-\omega_1)C_{jE} \\
&\left[\left(\frac{1}{8\eta_C^2V_T^2}-\frac{3}{32(V_{bi}-V_{BE})^2}\right)+A\left(\frac{1}{2\eta_C V_T}-\frac{1}{4(V_{bi}-V_{BE})}\right)\right]B \\
&+\frac{Z_{\pi,2\omega_2-\omega_1}}{Z_{IN,2\omega_2-\omega_1}+Z_{S,2\omega_2-\omega_1}}g_m\left(\frac{1}{8\eta_C^2V_T^2}+A\frac{1}{2\eta_C V_T}\right)B \qquad (18)
\end{aligned}
$$

where

$$
\begin{aligned}
A &= -\frac{(Z_{S,2\omega_2}+R_B+R_E)(b_2+j2\omega_2c_2)+R_Eg_2}{2[1+(Z_{S,2\omega_2}+R_B+R_E)(b_1+j2\omega_2c_1)+R_Eg_1]} \\
&\quad -\frac{(Z_{S,\omega_2-\omega_1}+R_B+R_E)(b_2+j(\omega_2-\omega_1)c_2)+R_Eg_2}{1+(Z_{S,\omega_2-\omega_1}+R_B+R_E)(b_1+j(\omega_2-\omega_1)c_1)+R_Eg_1} \qquad (19) \\
B &= V_{be,\omega_2}^2V_{be,\omega_1}^*
\end{aligned}
$$

The third-order output IM current in (18) has very similar form to the second-order one. The first term of (18) indicates that $I_{b,2\omega_2-\omega_1}$ is partially cancelled by $\frac{Z_{S,2\omega_2-\omega_1}+R_B+R_E}{Z_{IN,2\omega_2-\omega_1}+Z_{S,2\omega_2-\omega_1}}I_{c,2\omega_2-\omega_1}$, and it can be perfectly cancelled out for a matched ideality factors. The second term of (18) represents that the diffusion charge part of $I_{q,2\omega_2-\omega_1}$ is partially cancelled by $\frac{Z_{S,2\omega_2-\omega_1}+R_B+R_E}{Z_{IN,2\omega_2-\omega_1}+Z_{S,2\omega_2-\omega_1}}I_{c,2\omega_2-\omega_1}$. The third term shows that the distortion signal generated from the base-emitter depletion capacitance is again incompletely cancelled by some portion of that generated from i_C. The last one is non-cancelled g_m portion of $\frac{Z_{\pi,2\omega_2-\omega_1}g_m}{Z_{IN,2\omega_2-\omega_1}+Z_{S,2\omega_2-\omega_1}}$. It can be expressed at a low frequency as,

$$
\begin{aligned}
\frac{Z_{\pi,2\omega_2-\omega_1}}{Z_{IN,2\omega_2-\omega_1}+Z_{S,2\omega_2-\omega_1}}g_m &\cong \frac{r_\pi g_m}{r_\pi+g_mr_\pi R_E+R_E+R_B} \\
&\cong \frac{g_m}{1+g_mR_E}. \qquad (20)
\end{aligned}
$$

Symbol	Value	Symbol	Value
I_E	16 mA	β_{dc}	40
I_B	0.39 mA	β_{ac}	68
P_{in}	-60 dBm	Z_L	150 Ω
η_C	1.0	η_B	1.7
g_1	0.0089	Δf	1 MHz
g_2	0.1006	τ_B	8.72×10^{-13}
g_3	0.7620	C_{jE}	4.3×10^{-13}
c_1	9.63×10^{-13}	g_{m1}	0.6027
c_2	1.42×10^{-11}	g_{m2}	11.6350
c_3	2.05×10^{-10}	g_{m3}	149.7427
R_B	8 Ω	R_E	2 Ω
V_{bi}	1.627 V	V_{BE}	1.60 V

Table 1

The Model Parameters of HBT

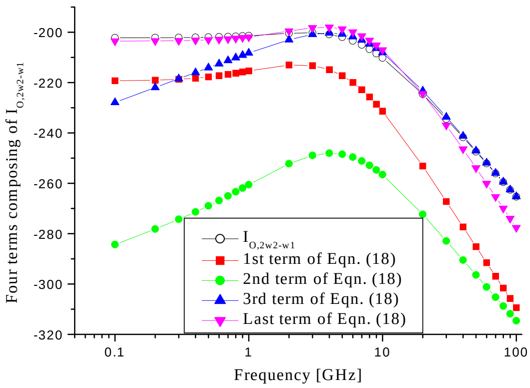

Fig. 3. Four terms composing $I_{O,2\omega_2-\omega_1}$ in (18).

It is identical to the low frequency equation and the emitter degeneration resistance is effective to reduce the last term.

For the analytical calculation of the nonlinear components of HBT, we used the model parameters of POSTECH built 3× 20 μm^2 emitter HBT. This device can deliver about 13 dBm of power. The parameters are summarized in Table 1. For the calculation, Z_S is adjusted to have impedance matching at the frequencies and input power is -60 dBm. Fig. 3 shows the frequency dependent values of the above 4 terms of $I_{O,2\omega_2-\omega_1}$ in (18). The cancellations between r_π and g_m, and C_{diff} and g_m nonlinearities is quite good for all frequencies. Therefore, the dominant nonlinear sources for all frequencies are C_{depl} and g_m. The third term becomes comparable to the last term at 2 GHz and above. At a low frequency (below 2 GHz), g_m nonlinearity with large degeneration resistor creates IM3. Between 2 ∼ 20 GHz, IM3 are generated by C_{depl} and g_m nonlinearities. At higher frequencies, the dominant source is C_{depl}. Complete cancellation of C_{diff} and r_π nonlinearities by g_m nonlinearity using identical ideality factors does not have any significant impact because they are rather small amount. We scanned η_C and η_B for a maximum IP3, HBT with $\eta_C = 1.0$ and $\eta_B = 2.0$ has maximum IP3 at 2 GHz (seen in Fig. 4).

Degeneration effects of the emitter and base resistances are also studied. Because $Z_{IN,2\omega_2-\omega_1}$ does not have any feedback term for an HBT with $R_E = 0$, the portion, $\frac{Z_{\pi,2\omega_2-\omega_1}}{Z_{IN,2\omega_2-\omega_1}+Z_{S,2\omega_2-\omega_1}}$, becomes relatively large, and IP3 level is degraded. The maximum IP3 of HBT is obtained at $R_E = 5\ \Omega$ and $R_B = 0\ \Omega$, which is 28.2 dBm. As R_E increases, IP3 level increases because the portion, $\frac{Z_{\pi,2\omega_2-\omega_1}}{Z_{IN,2\omega_2-\omega_1}+Z_{S,2\omega_2-\omega_1}}$ is reduced. But, larger R_E reduces not only the IM3 signal but also the fundamental signal, and a optimum value of R_E is about $5\ \Omega$ in our case. The emitter degeneration resistance is more effective than the base resistance.

As can seen from (18) and (19), the third order IM currents are dependent on the second harmonic impedance of $Z_{S,2\omega_2}$ and $Z_{S,\omega_2-\omega_1}$. We have calculated the IP3 of HBT using the source-termination at the second-harmonic frequency. The linearity of HBT is remarkably promoted for $Z_{S,2\omega_2} = 0$ and $Z_{S,\omega_2-\omega_1} = 0$. We also compute the IP3 levels of HBT with $Z_{S,2\omega_2} = \infty$ or $Z_{S,\omega_2-\omega_1} = \infty$, but it is degraded. Fig. 5 shows contour lines of IP3 level of HBT with $Z_{S,2\omega_2} = 0$ and $Z_{S,\omega_2-\omega_1} = 0$ for various η_C and η_B. The maximum IP3 of HBT with the source-termination is about 31 dBm for $\eta_C = 1.15$ and $\eta_B = 1.55$ which is 3.5 dB improvement.

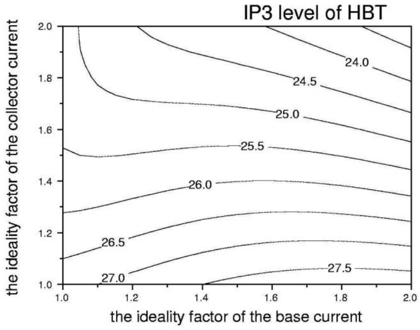

Fig. 4. The contour lines of IP3 level of an HBT using our model parameters with various η_C and η_B.

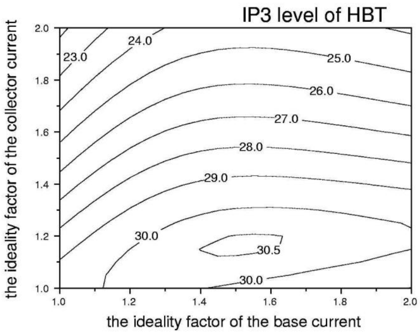

Fig. 5. The contour lines of IP3 level of an HBT with $Z_{S,2\omega_2} = 0$ and $Z_{S,\omega_2-\omega_1} = 0$ using our model parameters with various η_C and η_B.

V. Conclusions

To accurately understand the linear characteristics of HBT, we developed an analytical nonlinear HBT model using Volterra Series analysis. Our model considers four nonlinearities: r_π, C_{diff}, C_{depl}, and g_m. The analysis we present reveals that the cancellations between r_π and g_m, and C_{diff} and g_m nonlinearities are quite good for all frequencies. Further, C_{depl} and g_m are the main nonlinear sources of HBT. g_m can be linearized using degeneration resistors. The degeneration resistor, R_E, is more effective than R_B for reducing g_m nonlinearity. The C_{depl} nonlinearity becomes important at a high freequency. This analysis also provides the dependency of the source second harmonic impedance on the linearity of HBT. The IP3 of HBT improves considerably by setting the second harmonic impedance of $Z_{S,2\omega_2} = 0$ and $Z_{S,\omega_2-\omega_1} = 0$.

Acknowledgements

This work was supported in part by the Agency for Defense Development and the Brain Korea 21 Project of the Ministry of Education.

References

[1] Christopher T. M. Chang and Han-Tzong Yuan, "GaAs HBT's for High-Speed Digital Integrated Circuit Applications," *Proc.IEEE,* vol. 81, no. 12, pp. 1727-1743, 1993.
[2] P. M. Asbeck, M. F. Chang, J. J. Corcoran, J. F. Jensen, R. N. Nottenburg, A. Oki, and H. T. Yuan, "HBT Application Prospects in the US: Where and when?," *IEEE GaAs IC Symp. Tech. Dig.,* Monterey, CA., pp. 7-10, Oct. 1991.
[3] Guang-Bo Gao, David J. Roulston, and Hadis Morkoc, "Design Study of AlGaAs/GaAs HBTs," *IEEE Trans. Electron Devices,* vol. ED-37, no.5, pp. 1199-1208, May 1990.
[4] M. E. Kim, A. K. Oki, J. B. Camou, P. D. Chow, B. L. Nelson, D. M. Smith, J. C. Canyon, C. C. Yang, R. Dixit, and B. R. Allen, "12-40 GHz Low Harmonic Distortion and Phase Noise Performance of GaAs HBTs," *IEEE GaAs IC Symposium Digest,* pp. 117-120, Nov. 1988.
[5] Stephen A. Maas, Bradford L. Nelson, and Donald L. Tait, "Intermodulations in HBTs," *IEEE Trans. Microwave Theory and Tech.,* vol. MTT-40, no. 3, pp. 442-448, Mar. 1992.
[6] Taisuke Iwai, Shiro Ohara, Horoshi Yamada, Yasuhiro Yamaguchi, Kenji Imanishi, and Kazukiyo Joshin, "High Efficiency and High Linearity InGaP/GaAs HBT Power Amplifiers: Matching Techniques of Source and Load Impedance to Improve Phase Distortion and Linearity," *IEEE Trans. Electron Devices,* vol. ED-45, no. 6, pp.1196-1200, June 1998.
[7] K. W. Kobayashi, J. C. Cowles, L. T. Tran, A. Gutierrez-Aitken, M. Nishimoto, J. H. Elliott, T. R. Block, A. K. Oki, and D. C. Streit, "A 44-GHz-High IP3 InP HBT MMIC Amplifier for low DC Power Millimeter-wave Receiver Applications," *IEEE Journal of Solid-State Circuits,"* vol. 34, no. 9, pp. 1188-1194, Sept. 1999.
[8] Apostolos Samelis and Dimitris Pavlidis, "Mechanisms Determining Third Order Intermodulation Distortion in AlGaAs/GaAs HBTs," *IEEE Trans. Microwave Theory and Tech.,* vol. MTT-40, No. 12, pp. 2374-2380, Dec. 1992.
[9] J. Lee, W. Kim, T. Rho, and B. Kim, "Intermodulation Mechanism and Linearization of AlGaAs/GaAs HBT's," *IEEE Trans. on Microwave Theory and Tech.,* vol. MTT-45, no. 12, pp. 2065-2072, Dec. 1997.
[10] Nan Lei Wang, Wu Jing Ho, and J. A. Higgins, "AlGaAs/GaAs HBT Linearity Characteristics," *IEEE Trans. Microwave Theory and Tech.,* vol. MTT-42, no. 10, pp. 1845-1850, Oct. 1994.
[11] Peter Asbeck, "HBT Linearity and Basic Linearization Approaches," *IEEE MTT-S Int. Microwave Symp. Workshop,* Baltimore, Maryland, June 1998.
[12] M. Iwamoto, T. S. Low, C. P. Hutchinson, J. B. Scott, A. Cognata, X. Qin, L. H. Camnitz, P. M. Asbeck, and D. C. D'Avanzo, "Influence of Collector Design on InGaP/GaAs HBT Linearity," *IEEE MTT-S Int. Microwave Symp. Dig.,* Boston, MA, pp. 757-760, Jun. 2000.
[13] W. Kim, S. Kang, K. Lee, M. Chung, Y. Yang, and B. Kim, "The Effects of Cbc on the Linearity of AlGaAs/GaAs Power HBT," *IEEE Trans. on Microwave Theory and Tech.,* vol. MTT-49, no. 49, pp. 1270-1276, Jul. 2001.
[14] Stephen A. Maas, *Nonlinear Microwave Circuits,* Artech House, Norwood, MA, 1988.